Lawrence Berkeley National Laboratory

Title
BETA-DECAY ASYMMETRY FROM THE DECAYS OF ORIENTED 52Mn AND 60Co

Permalink
https://escholarship.org/uc/item/98r1884w

Authors
Hung, S.T.-C.
Krane, K.S.
Shirley, D.A.

Publication Date
1975-04-01

0 0 0 J 4 2 0 3 | 9 3

RECEIVED

BERKELEY LABORATORY

JUL 18 1975

LIBRARY AND
DOCUMENTS SECTION

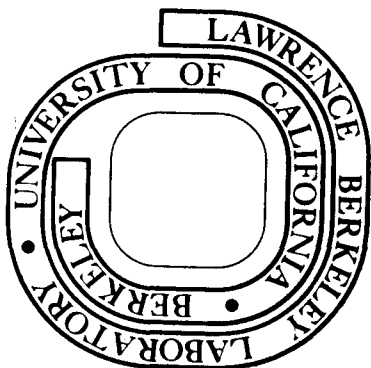# BETA-DECAY ASYMMETRY FROM THE DECAYS OF ORIENTED ^{52}Mn AND ^{60}Co

S. T.-C. Hung, K. S. Krane, and D. A. Shirley

April 1975

DISCLAIMER

BETA-DECAY ASYMMETRY FROM THE DECAYS OF

ORIENTED ^{52}Mn AND ^{60}Co*

S. T.-C. Hung,[†] K. S. Krane,[‡] and D. A. Shirley

Department of Chemistry and
Lawrence Berkeley Laboratory
University of California
Berkeley, California 94720

ABSTRACT

The beta decay of ^{52}Mn has been investigated by measuring the angular distribution asymmetry of the positrons emitted from ^{52}Mn oriented at low temperatures. The ^{52}Mn nuclei were polarized in an iron lattice and cooled by thermal contact with an adiabatically demagnetized paramagnetic salt. The positron asymmetry was determined by means of two independent techniques: the positrons were detected directly using high-purity germanium detectors and indirectly using NaI detectors to observe the annihilation gamma rays. These two techniques yielded a consistent result for the asymmetry, corresponding for this allowed decay to a ratio of the Fermi to Gamow-Teller matrix elements of $y = C_V M_F/C_A M_{GT} = -0.144 \pm 0.006$. An auxiliary experiment on ^{60}Co gave a beta asymmetry $A = -0.971 \pm 0.034$, in excellent agreement with the theoretical value of -1 expected for maximal parity violation.

I. INTRODUCTION

The study of the angular distribution of radiation emitted by oriented nuclei has proven to be a powerful and convenient means of deducing the properties of nuclear radiation fields, in particular their multipole character. In the case of allowed beta decay, such studies can be analyzed to yield the ratio of the Fermi (F) to Gamow-Teller (GT) matrix elements in the beta decay, from which ratio one can deduce in turn the degree of isospin mixing in the nuclear states (isospin selection rules forbid the emission of Fermi-type decays between low-lying states of pure isospin) and the magnitude of the charge-dependent nuclear matrix elements. Comprehensive reviews of the theoretical background necessary for interpretation of the results of this type of experiment, as well as summaries of experimental results, may be found in the works of Schopper[1] and of Wu and Moskowski.[2] The present report contains a description of a measurement of the angular distribution asymmetry in the allowed positron beta decay of oriented ^{52}Mn.

A compelling justification for undertaking a more precise determination of the F/GT ratio is based on the search for evidence of violations of fundamental symmetries in nuclei. In particular, in recent years numerous experimental studies have been made to search for evidence of parity (P) and time-reversal (T) violation in nuclei. Although no direct evidence for T violation has yet been obtained, indirect evidence results from the observation of CP-violation in the K_0 decay,[3] and there is speculation as to whether this effect arises from T violation in weak or electromagnetic interactions. In the case of allowed beta decay, T violation would be manifest as a complex phase of the F/GT ratio;

furthermore, as the size of the T-violating observable is proportional to $y/(1+y^2)$, where y is the ratio of Fermi to Gamow-Teller amplitudes, it is advisable to choose a case for investigation in which there is reasonable interference between the F and GT terms. Previous determinations of the ratio y in ^{52}Mn have not been in good agreement, and the possibility that a large value of y might make ^{52}Mn a favorable candidate for an investigation of T violation in beta decay has in part prompted the present remeasurement.

The F/GT ratio y may be determined from a measurement of the angular distribution anisotropy of beta particles relative to an axis of nuclear polarization. This may be implemented either (1) by observing the anisotropy of beta emission relative to the nuclear polarization axis (using an external polarizing field applied to nuclei cooled to ultralow temperatures[4]), or (2) by observing the angular correlation between the direction of beta emission (from an unpolarized nuclear state) and the direction of a subsequent coincident gamma ray, whose circular polarization must be detected.[5] Each of these two techniques suffers from serious difficulties, mostly involving the extraction of the "true" beta-ray angular distribution parameters from the observed angular distributions (i.e., correcting for background effects and determining analyzing efficiencies and experimental geometries). These difficulties are reflected in the non-statistical scatter of the results of measurements of the parameter y determined at various laboratories using either of the two techniques.

The circular polarization technique suffers particularly from the low efficiencies associated with coincidence counting and circular

polarization analysis. A significant drawback of the nuclear orientation
technique is the electron scattering from the metallic apparatus, necessary
to achieve ultralow temperature nuclear orientation, in the vicinity of
the sample. At best one hopes that the two methods will serve somewhat
to complement each other, and a complete determination of the parameters
of allowed decays should represent results from both methods. Unfortunately,
the experimental activity in this area, particularly as regards application
of the nuclear orientation technique, was largely confined to a few years
immediately subsequent to the discovery of parity violation in weak interactions
(by means of the first successful experimental study of beta emission
from polarized nuclei.[6]) In the intervening years, advances in particle
detectors, low-temperature technology, and nuclear polarization techniques
have provided an impetus for reapplying the nuclear orientation technique
to this problem. The present report describes determinations of the
positron beta-ray asymmetry in the decay of oriented ^{52}Mn employing two
independent and somewhat novel detection methods: (1) use of a long-
focusing solenoid to guide the positrons to an intrinsic Ge detector,
and (2) the coincident detection of the two positron annihilation photons.
The first method was used in a series of experiments that were completed
in 1972. The resulting value of $y = C_V M_F / C_A M_{GT}$ was much larger in
magnitude than any of the published values. Although we were very
confident that this result was correct, especially because a large
asymmetry was present even in the raw data, we nevertheless felt it
prudent to delay publication until an independent confirmation could be
made. Consequently the apparatus was rebuilt and another experiment
was carried out using the second method.

The theory of this type of measurement is recapitulated briefly in Section II. Experiments are described in more detail in Section III. Section IV describes data analysis. The results are given in Section V and discussed in Section VI.

II. THEORY

The theory of allowed beta emission from polarized nuclei has been described in numerous reviews; for example, that of Schopper.[1] Radiation emitted from an oriented nucleus is in general described by

$$W(\theta) = \sum_k Q_k B_k U_k A_k P_k(\cos \theta) , \qquad (1)$$

where the Q_k are the solid angle correction factors, B_k are orientation parameters describing the degree of orientation of the emitting nuclear state, U_k are deorientation parameters which correct for the effect of unobserved intermediate radiations, A_k are angular distribution coefficients which depend on the properties of the observed radiation, and P_k are Legendre polynomials evaluated at the angle θ between the emission direction and the polarization direction. In the case of allowed beta emission, the angular distribution function becomes (assuming T invariance, maximal P violation and no second forbidden contributions):

$$W_\beta(\theta) = 1 + Q_1 B_1 A_1 \cos \theta , \qquad (2)$$

where (for a $\Delta I = 0$ transition),

$$A_1 = \frac{[b_1(01) + b_1(10)]F_1(01II) + b_1(11)F_1(11II)}{b_0(00) + b_0(11)} , \qquad (3)$$

where the beta particle parameters are as given by Alder, Stech, and Winther,[7] who also tabulate the F-coefficients. Here some care must be exercised in accounting for the phases involved in the calculation, and in fact one obtains an error in the phase of the odd-order terms of the angular distribution when using the above angular distribution coefficients with the orientation parameters B_k of Blin-Stoyle and Grace.[8] This point has been discussed in a recent tabulation of the orientation parameters.[9] Although the convention adopted is irrelevant with respect to the final result, the choice of the phase used in the present work permits the odd-order angular distribution coefficients A_k to be written in a manner analogous to the case of gamma-radiation, in terms of particle parameters (which are simply the multipole matrix elements for gamma rays) times F-coefficients.

The angular distribution parameter reduces directly to

$$A_1 = \frac{2}{3}\frac{v}{c}\frac{yF_1(01II) + F_1(11II)}{1 + y^2} \tag{4}$$

where $y = C_V M_F / C_A M_{GT}$.

Since the experiment actually measures a continuous beta spectrum, the dependence on the beta-particle energy E must be included, and we consider then a correlation function $W_\beta(\theta,E)$ of the form

$$W_\beta(\theta,E) = N(E)(1 + Q_1 B_1 A_1 \cos\theta) \tag{5}$$

where N(E) gives the probability of beta emission between the energies E and E + dE

$$N(E) = N_0 E\sqrt{E^2 - 1} (E_0 - E)^2 F(Z,E) \quad , \tag{6}$$

with the energy E and end-point energy E_0 measured in units of $m_e c^2$. The beta particle kinetic energy is thus equal to $E - 1$, and the ratio v/c is given by $\sqrt{E^2 - 1}/E$.

In the present work, the angular distribution of the allowed beta emission from ^{52}Mn has been observed, and similar studies of the beta emissions from ^{58}Co and ^{60}Co were done for calibration and checks on the apparatus. The relevant features of the decay schemes of these isotopes are shown in Figures 1-3.[10] In Table I we summarize for convenience some of the relevant parameters of the decays. The hyperfine splitting Δ (the energy difference between adjacent magnetic substates) is obtained as $\Delta = \mu H/I k_B$, where μ is the nuclear moment (in nuclear magnetons μ_N), H is the hyperfine magnetic field of the impurity in an iron host lattice, and k_B is the Boltzmann constant. For a pure Gamow-Teller decay $I_i \rightarrow I_f$, such as that of ^{60}Co,

$$A_1 = \pm \frac{2}{3} \frac{v}{c} F_1(11I_fI_i) \quad . \tag{7}$$

where $\pm$ indicates $\beta^{\pm}$.

The orientation parameters of the parent level may be determined from the gamma-ray angular distribution using Eq. (1),

$$W_\gamma(\theta) = 1 + Q_2B_2U_2A_2P_2(\cos\theta) + Q_4B_4U_4A_4P_4(\cos\theta) \quad . \tag{8}$$

All of the isotopes studied emit pure E2 transitions which can be used for thermometry purposes.

III. EXPERIMENTAL

A. Low-Temperature Apparatus

The essential features of the low-temperature apparatus and the techniques of sample preparation were common to both the beta-particle and annihilation-photon experiments. The sample mounting, radiation detectors, and electronics were different for the two experiments and will be described separately.

The samples were cooled to temperatures in the range of 8 millikelvin (mK), corresponding to a ^{52}Mn polarization of 75%, by means of the adiabatic demagnetization of cerium magnesium nitrate. The dewar system employed to maintain the cryostat at temperatures of 1°K is shown in Figure 4. This system was originally designed with the possibility of a time-reversal experiment in mind. Such an experiment requires a β-γ coincidence measurement, and the sensitivity is maximized when the angle between the direction of emission of β and γ is 45°. For this reason the tail section of the dewars has been beveled at 45° to facilitate placement of the γ detectors.

The liquid nitrogen-liquid helium dewars system and 50 kOe cooling magnet were of conventional design. Further details of the construction may be found in a more detailed account of the positron detection experiments.[11]

B. Sample Preparation

The ^{52}Mn activity was obtained by proton irradiation of natural iron foils. In this way the activity is produced *in situ* in a ferromagnetic environment, obviating the need for chemical separation and the other sample preparation techniques normally associated with nuclear

orientation measurements. Foils of 10 mg/cm^2 (½ mil) thickness were employed; in the case of the positron measurement, the foils were rolled to 6 mg/cm^2. These thicknesses provided a reasonable compromise between the desirability of thin foils for reducing scattering of the beta particles and the corresponding reduced thermal conductivity of such thin foils, which may reduce the degree of nuclear polarization that can be attained.

The foils were irradiated with 32-MeV protons from the LBL 88-inch cyclotron. Currents of 5 μA were used, which were low enough to prevent burning of the foils. The activity was produced by means of the reaction

$$^{54}Fe(p,3n)^{52}Co \xrightarrow{\beta^+} {}^{52}Fe \xrightarrow{\beta^+} {}^{52}Mn \quad .$$
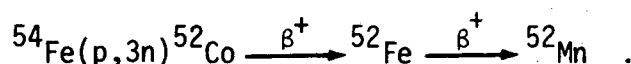
The ^{52}Co and ^{56}Co activities also produced did not interfere with the experiment; the 18-hour ^{55}Co was allowed to decay away, and the ^{56}Co activity was considerably weaker than the ^{52}Mn.

The ^{60}Co and ^{58}Co samples were produced from activity obtained commercially in HCl solution. The activity was evaporated onto iron foils and reduced under H$_2$. The foils were melted and then rolled to thicknesses in the range of 10 mg/cm^2 (½ mil).

All foils were annealed prior to being soldered to the cold-finger of the apparatus using (non-superconducting) Bi-Cd solder.

C.   Apparatus

1. Positron Measurements.

A schematic representation of the lower tail section of the cryostat is shown in Figure 5. An intrinsic germanium detector of 0.8 mm

thickness (0.5 mm depletion depth) was used for the positrons. The area of the detector was 0.63 cm^2, and with the 0.64 cm diameter collimator, the solid angle subtended by the detector at the source was 0.03%.

The intrinsic Ge detector employed in the present work provided the advantage of the superior energy resolution normally associated with solid-state detectors, while not exhibiting the loss in performance which would have been characteristic of the more conventional lithium-drifted detectors when the detector housing was periodically warmed in order to change samples.

The principal difficulties associated with this type of experiment arise from either (a) the response of the detector to unwanted events, mainly gamma rays and Compton-scattered electrons, or (b) positrons which are back-scattered from the detector, resulting in incomplete energy deposition. The gamma response of the detector is minimized by using as thin a detector as possible. The Compton electrons are a potentially more serious problem; for every positron emitted in the ^{52}Mn decay, there are about nine high-energy gamma rays emitted. These gammas can Compton-scatter from the sample, the chamber walls, and the copper cold finger. The use of a long-focusing solenoid (which also provides the external polarizing field for the sample) serves to optimize the beta-particle detection efficiency relative to that of the Compton electrons. The magnetic field of the solenoid guides the beta particles from the source to the detector, while electrons which originate elsewhere spiral along the field lines and tend to be absorbed eventually by the cryostat walls or the detector collimator. The geometry was arranged such that the detector and source were each placed 2.5 cm in from the opposite

ends of the solenoid. The solenoid was operated at a field of 10.5 kOe.

The detector chamber provided a vacuum independent of the cryostat, a thin mylar entrance window for the positrons, and a detector mounting thermally anchored at 1°K. The performance of germanium detectors is at best unpredictable at temperatures below 10°K; optimum performance is generally obtained when the detector is warmed (as, for example, with a resistance heater) to temperatures of ca. 20°K. The intrinsic germanium detector employed in the present work operated well down to 1°K, but had a tendency to polarize (due to trapped charges) after a period of 12 hours. It was found that the application of a forward bias voltage of 1 - 2 volts was sufficient to sweep out the trapped charges.

The electronic system consisted of conventional linear pulse amplifiers and discriminators. The digitized positron energy spectra were written onto magnetic tape for subsequent computer analysis.

2. Annihilation Photon Measurements.

A schematic diagram of the lower tail section of the cryostat employed in the annihilation photon measurement is shown in Figure 6. Positrons emitted by the source were stopped in the 2-mm thick bottom cap of the cryostat tail section (a relatively smaller number which are stopped in the lower section of the cryostat wall may be taken into account in the calculation of the geometrical correction factors). The annihilation gives rise to two 511 keV photons emitted in opposite directions. These are collimated somewhat by means of the lead collimator shown in Figure 6; a sufficient amount of lead was used to prevent radiations from the sample from reaching the detectors directly. The two photons were further collimated by detecting the pair in coincidence

using a pair of 7.6 cm by 7.6 cm NaI(Tl) detectors. (In actuality two independent pairs of detectors were used to increase the rate of data accumulation; these pairs were oriented at right angles to one another.) The effectiveness of the shielding and collimation were tested by raising and lowering the sample relative to the detector and shielding assembly. The only change in the observed coincidence rate was that due to the change in solid angle subtended at the source by the end cap. Furthermore, the entire detector and shielding assembly could be raised or lowered by about 1 cm with no change in the count rate. The coincidence spectrum revealed only the presence of the 511 keV gamma ray, and thus the energy interval accepted by the single-channel analysis could be set quite wide with no fear of accepting spurious counts. Such widths are necessary to eliminate the possibility that changes in the applied polarizing field would affect the detector photomultiplier tubes and produce a gain shift in the energy analysis. Widths of the order of ± 200 keV were used, and no changes in count rate were observed with fields up to 3 kOe.

This arrangement eliminates a number of the difficulties associated with the direct measurement of the positrons, in particular: (1) back-scattering, since only those positrons which stop completely in the "detector" are counted; and (2) sensitivity of the solid-state detector to Compton electrons and photons, since this system has no sensitivity to either. However, these advantages are offset by a loss of the positron energy resolution -- all positrons are counted, regardless of energy, and the observed counting rate represents an average of the angular distribution over the positron energy range. Although this would appear to be a serious effect, the angular distribution function depends not directly

on the positron energy but rather on v/c, which varies relatively slowly
over the energy spectrum. Furthermore, the effects of scattering within
the source foil and of the magnetic field on the curvature of the positron
paths serve to reduce the number of low-energy positrons which reach the
scatterer; it is in the low-energy region that v/c varies most rapidly
with positron energy.

The samples were prepared as described in Section III.B. and were
soldered to an extension of the cold finger which was oriented at an
angle of 45° relative to the scatterer. Backscattering in the vicinity
of the source was reduced somewhat by hollowing out the inside of the
source holder. The samples were polarized by means of two mutually
perpendicular Helmholtz pairs, aligned so that one pair produced the
field shown as H_{app} in Figure 6 while the other could produce a field
normal to the plane of the figure. The latter situation was used to
provide a measure of $W_\gamma(90°)$ for the determination of the degree of
alignment of the nuclei, while the former field is that used for the
positron measurements, and provided a nuclear polarization direction
(in the plane of the foil) at 135° or 45° relative to the direction of
detection. In this geometry of sample and coils, the positrons were
emitted normal to the external polarizing field, and were thus subject
to considerable Lorentz forces. For this reason the magnitude of the
polarizing field was kept as small as possible. It was found that no
significant loss of polarization was obtained in fields down to 0.6 kOe,
if the sample was first saturated in a field of 2 kOe; however, applied
fields greater than 1 kOe resulted in substantial (> 50%) losses in
count rate, owing to the bending of the positrons' paths such that they

collided with the cryostat walls before reaching the bottom of the cryostat.

IV. PROCEDURE AND DATA ANALYSIS

A. β^+ Measurements

Following demagnetization, the sample was polarized in an external field of 10.5 kOe directed away from the beta detector. Six 10-minute runs were taken; after each run the detector was slightly forward-biased in order to sweep out the trapped charges and avoid polarization of the detector. The polarizing field was then reversed for an additional six 10-minute runs. Finally, the salt pill was warmed up to 1°K and three runs were taken with the field in each direction.

During the data accumulation, the sample temperature was monitored by observing the anisotropy of the 744 keV gamma ray with a Ge(Li) detector. During the experiment the temperature remained constant at 8 mK, corresponding to a polarization of 76%.

The theoretical beta anisotropy was given previously as

$$W_\beta(\theta = 0°) = 1 + \frac{v}{c} Q_1 \tilde{A}_1 B_1 \qquad (9)$$

where we have factored out the v/c dependence $(A_1 = \frac{v}{c} \tilde{A}_1)$. In order to extract the beta angular distribution from the observed spectra, a number of corrections were necessary. These are discussed below; the general effect of these corrections is to compensate for a difference between the "true" v/c and the "observed" v/c.

1. Compton Electrons.

If the detector is sensitive to Compton electrons from scattered gamma rays (or to the gamma rays themselves), an additional term is introduced into the angular distribution of the form $f_c W_\gamma$, where f_c is the fraction of events which arise from this source (estimated to be of the order of 10%) and W_γ is the gamma ray angular distribution, which we take to be represented by $W_\gamma(\theta = 0°)$. Thus the observed angular distribution W is given by

$$W = W_\beta + f_c W_\gamma ,\qquad (10)$$

and if we consider the difference in counting rates between the two field directions $\theta = 0°$ and $\theta = 180°$, we obtain

$$\frac{W(0°) - W(180°)}{2\bar{W}} = \frac{\beta Q_1 \tilde{A}_1 B_1}{1 + f_c} \qquad (11)$$

Here the warm isotropic counting rate is given by $\bar{W} = 1 + f_c$ ($W_\beta = W_\gamma = 1$ at high temperatures), and we have written $\beta = v/c$. Similarly,

$$\frac{W(0°) + W(180°)}{2\bar{W}} = \frac{1 + f_c W_\gamma}{1 + f_c} \qquad (12)$$

If W_γ is taken as the $0°$ gamma ray counting rate, then f_c may be determined and the appropriate correction applied to Eq. (11).

2. Pile-Up.

Pile-up can occur between Compton electrons and positrons (estimated to contribute about 1% of the observed intensity) or between annihilation photons and positrons (5%). The effect of this pile-up is to increase

the counting rate in the high-energy region of the spectrum. The relative importance of the annihilation photons in giving rise to this effect was evidenced in the failure to observe any similar effect of comparable magnitude in the ^{60}Co spectra which were used for calibration purposes. The effect of these pile-up contributions on the angular distribution is to introduce, into the energy region corresponding to β, a term corresponding to some lower β'. The contributions of the positron-Compton and positron-annihilation photon pile-up terms may then be written, respectively, as

$$W_{\beta e} = f_{\beta e}(1 + \beta' Q_1 B_1 \tilde{A}_1)W \quad , \tag{13}$$

$$W_{\beta \gamma} = f_{\beta \gamma}(1 + \beta'' Q_1 B_1 \tilde{A}_1) \quad , \tag{14}$$

where $f_{\beta e}$ and $f_{\beta \gamma}$ are the magnitudes of these pile-up contributions.

3. Backscattering.

The effect of those positrons which scatter out of the detectors without full energy deposition is to introduce, in the energy region corresponding to β, a contribution to the angular distribution corresponding to some *larger* β''', which we write as

$$W_s = f_s(1 + \beta''' Q_1 B_1 \tilde{A}_1) \quad . \tag{15}$$

The complete observed (renormalized) beta angular distribution may then be written as

$$W = W_\beta + f_c W_\gamma + W_{\beta e} + W_{\beta \gamma} + W_s \quad . \tag{16a}$$

$$= \frac{1 + \beta \alpha_1 + f_c W_\gamma + f_{\beta e} W_\gamma (1 + \beta' \alpha_1) + f_{\beta \gamma} (1 + \beta'' \alpha_1) + f_s (1 + \beta''' \alpha_1)}{1 + f} \tag{16b}$$

$$= 1 + \langle \beta \rangle \alpha_1 + \frac{(W_\gamma - 1)(f_c + f_{\beta e})}{1 + f} \tag{16c}$$

with $f = f_c + f_{\beta e} + f_{\beta \gamma} + f_s$, and $\alpha_1 = Q_1 B_1 \tilde{A}_1$, and where the average β is given by

$$\langle \beta \rangle = \beta \frac{1 + \frac{\beta'}{\beta} W_\gamma f_{\beta e} + \frac{\beta''}{\beta} f_{\beta \gamma} + \frac{\beta'''}{\beta} f_s}{1 + f} \tag{17}$$

As before, we then obtain

$$\frac{W(0°) - W(180°)}{2\overline{W}} = \frac{1 + \langle \beta \rangle \alpha_1}{1 + f} \tag{18}$$

and

$$\frac{W(0°) + W(180°)}{2\overline{W}} = \frac{1 + (W_\gamma - 1)(f_c + f_{\beta e})}{1 + f} \quad . \tag{19}$$

Although it is impossible to separate the contributions from the various corrections, the overall effect of the factor f may be estimated from Eq. (19) since $(W_\gamma - 1)$ is reasonably small (approx. -0.3). If one then assumes that the pile-up and backscattering tend to cancel one another's effect on $\langle \beta \rangle$, the positron spectrum may be renormalized to facilitate extraction of the asymmetry parameter.

One additional correction which must be applied involves the calculation of the solid-angle correction factor Q_1, which in general depends on the strength of the field and on the positron velocity, since the focusing effect of the long solenoid will be different for positrons having different velocities. The effective solid angle is of order π (25%) for the range of beta energies considered in this work, with the half-angle of the detector ranging from 65° ($\beta = 0.6$) to 52° ($\beta = 0.88$). The computed values of the solid-angle correction factor varied between 0.7 and 0.8 for the experimental geometry.

B. Annihilation Photon Measurements

Following demagnetization, the sample was polarized in an external field of 2 kOe oriented at 90° relative to the direction of the gamma-ray detector (and also of the positron absorber). The gamma-ray anisotropy in this configuration was used to deduce the polarization of the sample. The current in that pair of coils was then reduced to zero and the current in the other pair turned up such that the 45° field (relative to the positron absorber) was 2 kOe. This field was sufficient to saturate the internal field of the iron foil; however it was also sufficiently large to prevent a large number of positrons from reaching the absorber due to deflection by the field. The field was then reduced to 0.6 kOe; this magnitude was determined empirically as a fair compromise between the necessity of maintaining a reasonable degree of polarization in the sample and the desirability of having the smallest possible curvature of the positron's path.

Even at these low applied fields, this curvature was considerable.

In general the result of such curvature is to prevent low-velocity positrons from reaching the bottom absorber, since they now are bent into paths of large curvature and collide with the walls. The entire problem is somewhat more complex, however, since one must not only consider the effect on the polar angle θ (nominally 45°) but also on the azimuthal angle φ. We have computed the positron paths numerically from the theoretical expressions for the off-axis fields of a Helmholtz pair; the result of this computation gives us a relationship between the polar angle θ and positron energy, and also a lower cut-off energy E_{min}, below which the geometry of our experiment would prevent the annihilation photons from being counted.

Assuming the polar angle can be represented by a deviation angle α relative to 45° or 135° (depending on the direction of the hyperfine field), we compute the asymmetry

$$\alpha = \frac{W(\uparrow) - W(\downarrow)}{W(\uparrow) + W(\downarrow)} \quad , \tag{20}$$

where the arrows indicate symbolically the applied field direction. For the geometry of the present experiment

$$\alpha = \frac{W(45° - \alpha) - W(135° + \alpha)}{W(45° - \alpha) + W(135° + \alpha)} \tag{21}$$

using Eq. (5) for the beta angular distribution and averaging over the beta energies (due to the lack of energy resolution), we obtain

$$\alpha = \frac{\int N(E)dE \; Q_1 B_1 A_1 \; \cos45°(\sin\alpha + \cos\alpha)}{\int N(E)dE} \qquad (22a)$$

$$= \frac{B_1 \tilde{A}_1 \; \cos45° \int N(E)dE \frac{v}{c} Q_1(\sin\alpha + \cos\alpha)}{\int N(E)dE} \qquad (22b)$$

We have taken $\alpha = \alpha(E)$, and have written $A_1 = \tilde{A}_1 \frac{v}{c}$. The integrals are carried out from some cut-off energy E_{min} to the beta end-point energy E_{max}. The energy E_{min} is determined by the orbital considerations discussed above, with a small additional correction applied to account for absorption within the source. In evaluating the solid-angle correction Q_1 we assume our absorber to be a black disk.

V.   RESULTS

A.   Positron Measurement

The result of the ^{60}Co measurement, following application of corrections as described in Section IV.A., was

$$\tilde{A}_1 = 0.615 \pm 0.021,$$

which compares well with the expected value

$$\tilde{A}_1 = -\frac{2}{3} F_1(1145) = 0.633$$

The above experimental value represents a least-squares fit over the beta energy range 140 keV to 280 keV, and the quoted uncertainty is three times the standard deviation of the least-squares fit. Figure 7 shows the raw and the corrected data. The good agreement between theory and experiment in the case of ^{60}Co lends confidence to the ^{52}Mn results.

The raw and the corrected data for ^{52}Mn are shown in Fig. 8. A similar least-squares fit of the corrected asymmetries between 105 keV and 560 keV yielded

$$\tilde{A}_1 = -0.250 \pm 0.007 \quad .$$

Again the uncertainty represents three times the standard deviation of the least-squares fit.

B. Annihilation Photon Measurement

The annihilation photon (β^+) counting rates were determined for the two opposite field directions and the asymmetry computed according to Eq. (20). The orientation parameter B_1 was determined from the γ-ray anisotropy measurement, and this in turn permitted the parameter B_1 to be computed. The asymmetries were corrected for the B_1, and the average values obtained were

$$^{58}\text{Co} \quad a/B_1 = 0.060 \pm 0.002$$
$$^{52}\text{Mn} \quad a/B_1 = 0.074 \pm 0.006$$

These results were corrected as described above, with an additional small correction included in the case of ^{58}Co to account for an apparent small deviation ($\sim 5°$) of the plane of the foil from 45° (as determined from the γ-ray anisotropy). The corrected angular distribution parameters are then

$$\tilde{A}_1(^{58}\text{Co}) = -0.217 \pm 0.018$$

$$\tilde{A}_1(^{52}\text{Mn}) = -0.235 \pm 0.027$$

The results for ^{58}Co are in substantial agreement with the previous results of Andrews et al.[12] ($\tilde{A}_1 = -0.243 \pm 0.007$) and indicate that the

various correction factors have been reasonably well accounted for. The present results indicate $y = +0.016 \pm 0.016$ for ^{58}Co, which is consistent with previous studies.[12]

VI. DISCUSSION

Assuming maximal parity violation, time-reversal invariance, and vanishing second-forbidden contributions, the present results indicate a Fermi/Gamow-Teller mixing ratio of

$$y = -0.144 \pm 0.006 \quad (\beta^+)$$
$$y = -0.131 \pm 0.024 \quad (\gamma\gamma)$$

where β^+ and $\gamma\gamma$ refer to the positron and annihilation photon measurements, respectively.

There have been numerous previous studies of the allowed beta decay of ^{52}Mn, using both the positron asymmetry[13,14] and circular polarization techniques.[15-21] These results and the corresponding deduced values of y are summarized in Fig. 9. As can be seen, there is considerable non-statistical scatter in the various results, with the present results showing evidence for the largest amount of Fermi/Gamow-Teller mixing yet attained.

The nuclear polarization results (refs. 13, 14 and the present work) strongly favor non-vanishing negative values of y, while there seems to be no consistent trend among the results of the circular polarization correlations. [These results are interpreted as

$$W_{\beta\gamma_p}(\theta) = 1 + \frac{v}{c} \tilde{B}_1(\beta) A_1(\gamma)\cos\theta , \tag{23}$$

where $\tilde{B}_1(\beta)$ is the angular orientation parameter describing the beta decay

$$\tilde{B}_1(\beta) \;=\; \frac{2}{3}\,\frac{-y\,F_1(01II) + F_1(11II)}{1 + y^2} \tag{24}$$

in analogy with Eq. (4)]. Although several of the circular polarization results[17,19,20] agree with the negative y-values obtained in the polarized nuclei experiments, the most precise of the quoted circular polarization results[18,21] indicate vanishing y-values.

In comparing our result for ^{52}Mn with the earlier nuclear polarization measurements,[13,14] we note that the agreement is actually relatively good considering the differences in experimental conditions. Although the values of y deduced from the earlier work was lower than ours by a factor of 3, the observed values of A_1 were lower by only a factor of 1.6. Our experiments had the great advantage of being carried out in a ferromagnetic metal, in which high thermal conductivity ensured a uniform sample temperature. The hyperfine Hamiltonian was both simple and well-known, and the warm-up rate was very low. The earlier nuclear polarization studies were done in the paramagnetic salt CMN -- the only lattice then available. There are two inequivalent sites for the divalent ions in this material with different and rather complicated hyperfine Hamiltonians. The poor thermal conductivity and rapid heat-leak rates, which would cause the outer layers of the CMN crystals (from which the positrons that reached the counters were emitted) to be warmer than the rest, would reduce the apparent positron asymmetry below its true value. In the hundreds of nuclear orientation experiments that have been carried out in our Laboratory

using both paramagnetic salts and ferromagnetic metals as hosts, we have observed just this kind of discrepancy many times.[22] An attenuation factor of ~ 1.6 is about what we would have expected from the paramagnetic salt work, under the circumstances of the early experiments.

The variations in the circular polarization results are more difficult to reconcile. The presence of impurity activities is unlikely to contribute to the differences, since the $^{52}Cr(p,n)^{52}Mn$ reaction used in the circular polarization studies produces no long-lived positron-emitting activities other than ^{52}Mn. Although there are variations in the beta- and gamma-ray discriminator levels used in the circular polarization work, there seems to be no direct correlation between the discriminator settings and the experimental asymmetry.

In comparing the nuclear polarization results with the circular polarization data several facts are inescapable:

(1) The nuclear polarization method is very direct. A large asymmetry was obvious by visual inspection of the raw data. Any experimental problems tend to decrease the apparent asymmetry. The total range of all nuclear polarization results for ^{52}Mn (a factor of 1.6 in the observed asymmetry) is well understood.

(2) The β-γ circular polarization correlation method is not as direct, requiring a large correction factor to go from raw data to the asymmetry parameter A_1. The measured A_1 values in the literature scatter badly.

(3) Finally, the nuclear polarization method is less susceptible in this case to any possible error in formulation of the theory.

The magnitude of the observed asymmetry is much larger than would be expected from a pure Gamow-Teller transition: there must be a substantial Fermi admixture.

Although the present results do not shed additional light on the conflicting circular-polarization values in the literature for the Fermi/ Gamow-Teller mixing ratio of the positron decay of ^{52}Mn, they do indicate the presence of a non-vanishing Fermi matrix element. The Fermi amplitudes would vanish for strict obedience to the isospin selection rules ($M_F = 0$ when $\Delta T \neq 0$; here $\Delta T = 1$), although it is perhaps doubtful that T can be regarded as a good quantum number for as heavy a nucleus as ^{52}Mn. The Fermi amplitude gives a measure of the degree of isospin impurity in the nuclear states, or, equivalently, of the size of the Coulomb matrix element which distorts the symmetry between protons and neutrons. While the scatter of the experimental results to date is large, the present results do provide evidence in support of a rather large Fermi amplitude. In particular, based on the presently deduced value of y, a Fermi matrix element $M_F = 0.017$ is deduced, with a corresponding isospin mixing amplitude of $\alpha = 0.009$ and a Coulomb matrix element $H_c = 70$ keV (these quantities are defined and discussed by Schopper[1]). Thus the present results suggest · that the ^{52}Mn decay would be a reasonable candidate for a future study of time-reversal invariance in beta decay.

-25-

FOOTNOTES AND REFERENCES

*Work performed under the auspices of the U. S. Energy Research and Development Administration.

†Present address: Student Affairs Office, School of Medicine, University of California, San Francisco 94143.

‡Present address: Department of Physics, Oregon State University, Corvallis, Oregon 97330.

1. H. F. Schopper, Weak Interactions and Nuclear Beta Decay (North-Holland, Amsterdam, 1966).

2. C. S. Wu and S. Moskowski, Beta Decay (Wiley, New York, 1966).

3. J. H. Christenson, J. W. Cronin, V. L. Fitch and R. Turlay, Phys. Rev. Letters 13, 138 (1964).

4. S. R. deGroot, H. A. Tolhoek and W. J. Huiskamp, in Alpha-, Beta-, and Gamma-Ray Spectroscopy, edited by K. Siegbahn (North-Holland, Amsterdam, 1965), p. 1199.

5. H. Frauenfelder and R. M. Steffen, in Alpha-, Beta-, and Gamma-Ray Spectroscopy, edited by K. Siegbahn (North-Holland, Amsterdam, 1965), p. 997.

6. C. S. Wu, E. Ambler, R. W. Hayward, D. D. Hoppes, and R. P. Hudson, Phys. Rev. 105, 1413 (1957).

7. K. Alder, B. Stech and A. Winther, Phys. Rev. 107, 728 (1957).

8. R. J. Blin-Stoyle and M. A. Grace, in Handbuch der Physik, edited by S. Flügge (Springer-Verlag, Berlin, 1957), Vol. XLII, p. 555.

9. K. S. Krane, Nuclear Data Tables 11, 407 (1973).

10. C. M. Lederer, J. M. Hollander and I. Perlman, Table of Isotopes (Wiley, New York, 1967).

Table I. Relevant Decay Properties of ^{52}Mn, ^{58}Co, ^{60}Co

Parent Nuclide	I_i	I_f	μ^a (μ_N)	H^b (kOe)	Δ (mk)	End point energy (keV)	$F_1(01 I_f I_i)$	$F_1(11 I_f I_i)$
^{52}Mn	6	6	+3.062	-227.0	4.24	575	1.732	-0.134
^{58}Co	2	2	+4.044	-287.7	21.3	474	1.732	-0.354
^{60}Co	5	4	+3.799	-287.7	8.01	313	--	-0.949

[a]V. S. Shirley, in Proceedings of the International Conference on Hyperfine Interactions Studied in Nuclear Reactions and Decay, edited by E. Karlsson and R. Wappling, (Uppsala, Upplands Grafiska AB, 1974).

[b]T. Koster and D. A. Shirley, in Hyperfine Interactions in Excited Nuclei, edited by G. Goldring and R. Kalish (Gordon and Breach, New York, 1971), p. 1239.

FIGURE CAPTIONS

Fig. 1. Partial decay scheme of ^{52}Mn.

Fig. 2. Decay scheme of ^{58}Co.

Fig. 3. Partial decay scheme of ^{60}Co.

Fig. 4. A schematic diagram of the dewar system. OVJ - Outer Vacuum
Jacket, in which aluminized mylar "superinsulation" was used to
reduce radiation into the dewars; IVJ - Inner Vacuum Jacket; 77°K
bath - liquid nitrogen at atmospheric pressure; 4.2°K bath - liquid
helium at atmospheric pressure; 1°K bath - liquid helium pumped to a
pressure of 60 microns.

Fig. 5. Cryostat tail section used for direct measurement of positron
asymmetry. The paramagnetic salt (CMN) is in contact with a series
of copper metal fins, which eventually become the cold finger to
which the sample is attached. The sample itself is soldered to a
copper wire loop which is in turn attached to the cold finger. The
intrinsic Ge detector is housed in its own vacuum chamber. The
solenoid (2.5 cm diameter by 14 cm length) provides a magnetic field
parallel to the axis of the cryostat; this field serves to polarize
the sample as well as to focus the positrons toward the detector.

Fig. 6. Cryostat tail section, detector, and shielding used for indirect
measurement of positron asymmetry by annihilation radiation. Positrons
stopping in the bottom of the cryostat create two 511-keV photons
emitted in opposite directions. These are detected in coincidence
(second detector not shown). Lead shielding prevents radiation from
the source itself from reaching the detector. For annihilation which
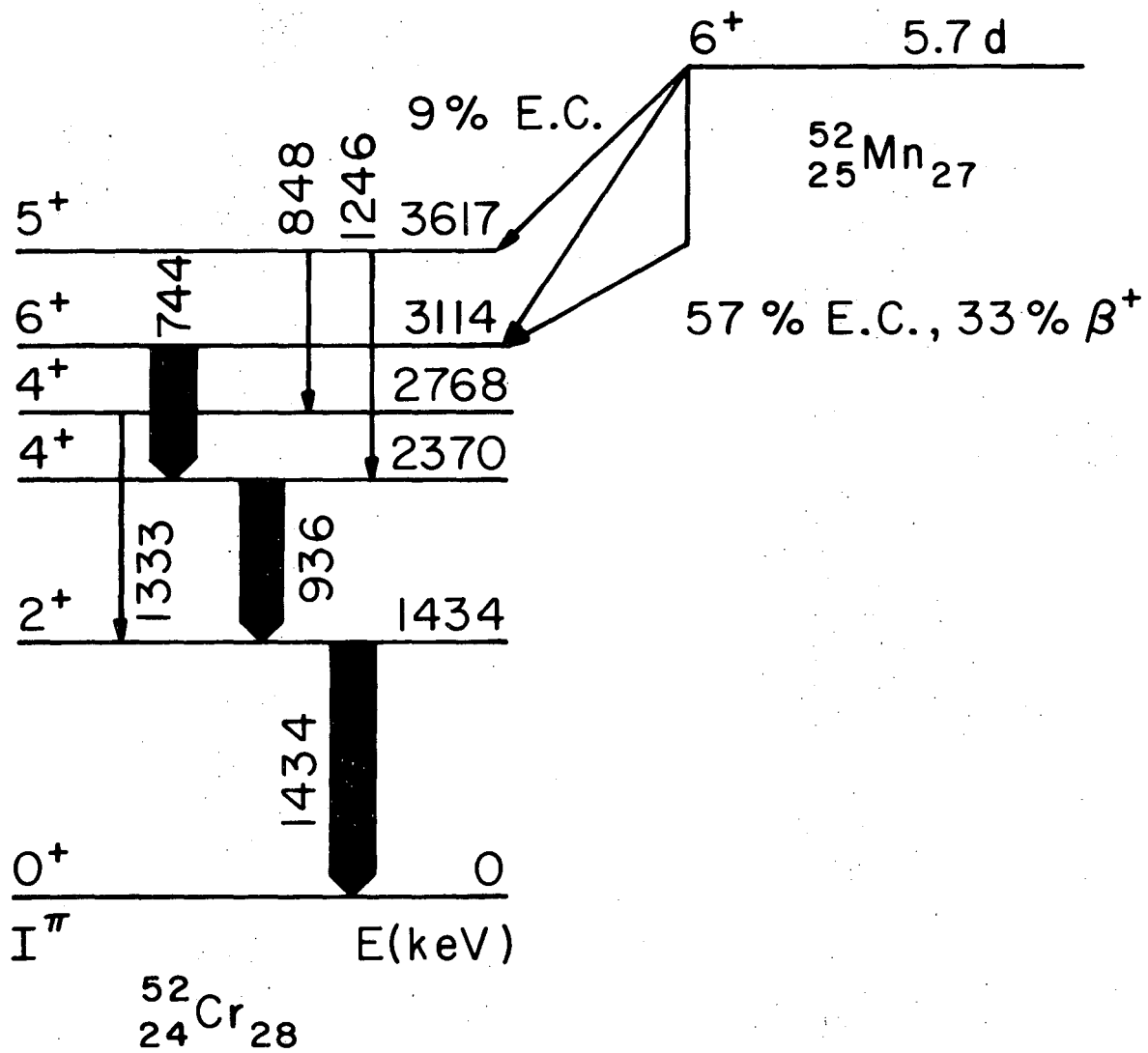takes place within the source, one of the photons may have a small

probability of reaching one of the counters, as shown, however the other photon would have zero probability of being counted, and hence this coincidence requirement serves to strengthen the collimation conditions.

Fig. 7. Raw and corrected beta asymmetries from the decay of polarized ^{60}Co. The lower portion of the figure shows the actual spectra recorded for two orientations of the applied field and the isotropic warm counts. The upper portions shows the corrected asymmetries in terms of the beta angular distribution parameter A_1. The horizontal bar shows the energy region used in arriving at the final result.

Fig. 8. Raw and corrected positron asymmetries from the decay of polarized ^{52}Mn. See caption to Fig. 7.

Fig. 9. Summary of results to date on the Fermi to Gamow-Teller mixing ratio y in the ^{52}Mn decay. The author's quoted results for the beta angular distribution coefficient $(\tilde{A}_1(\beta)$, from experiments with polarized nuclei) and beta angular orientation coefficient $(\tilde{B}_1(\beta)$, from circular polarization experiments) are shown on the theoretical curves of $\tilde{A}_1$ or $\tilde{B}_1$ vs. y (these curves are linear for small y). The corresponding deduced values of y are shown on the left.

References are:
a - Boehm (1958), ref. 15
b - Boehm (1962), quoted in ref. 16
c - Bloom et al (1962), ref. 16
d - Mann et al (1965), ref. 18
e - Pingot (1971), ref. 21
f - Postma et al (1958), ref. 13
g - Sawyer (1968), ref. 20
h - Ambler et al (1958), ref. 14
i - Behrens (1967), ref. 19
j - Daniel et al (1962), ref. 17
k - Present work, $\gamma\gamma$
l - Present work, β^+

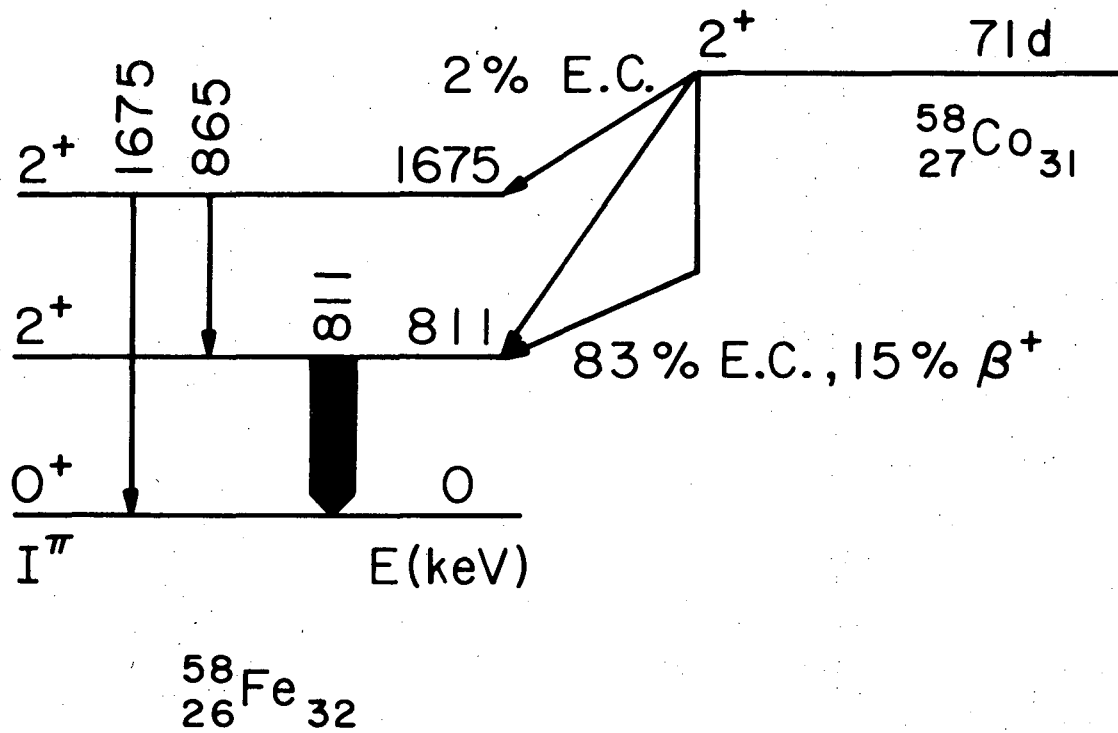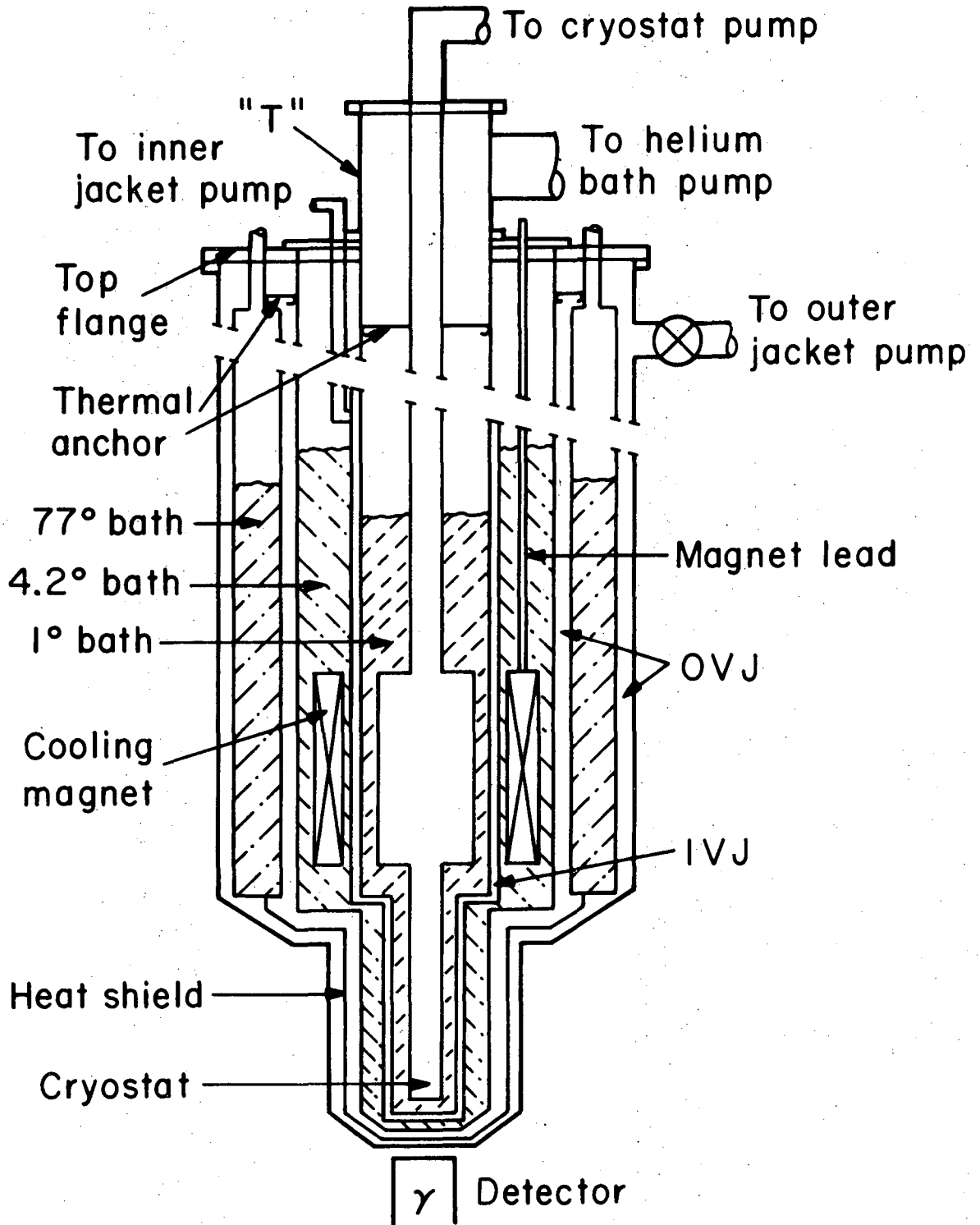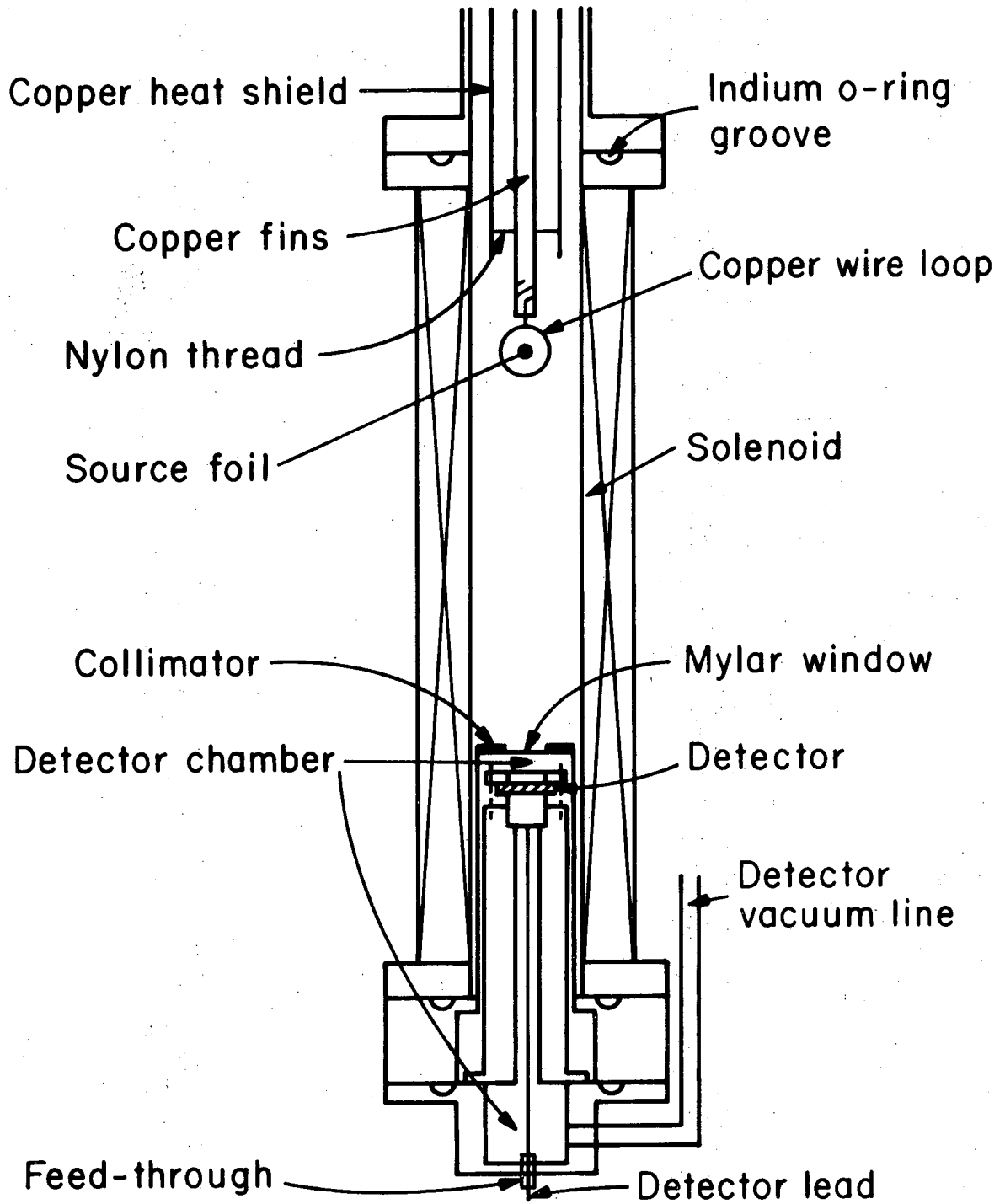Fig. 1

XBL 754-2615

Fig. 2

Fig. 3

XBL 754-2617

Fig. 4

XBL754-2618

Copper heat shield

Indium o-ring groove

Copper fins

Copper wire loop

Nylon thread

Source foil

Solenoid

Collimator

Mylar window

Detector chamber

Detector

Detector vacuum line

Feed-through

Detector lead

XBL 754- 2619

Fig. 5

Outer dewar
Cold-finger
Cryostat
Source

H_{app}

β^+

45°

Lead

511 keV photon

Na I detector

Ge(Li) detector

XBL 754-2620

Fig. 6

XBL754-2621

Fig. 7

Beta energy (keV)

XBL 754-2622

Fig. 8

XBL754-2623

Fig. 9

0 0 0 0 4 2 0 3 2 1 1